

Metal-Insulator Transition of the $\text{LaAlO}_3\text{-SrTiO}_3$ Interface Electron System

Y. C. Liao,¹ T. Kopp,¹ C. Richter,¹ A. Rosch,² and J. Mannhart¹

¹*Experimental Physics VI, Center for Electronic Correlations and Magnetism,
Institute of Physics, University of Augsburg, D-86135 Augsburg, Germany*

²*Institute of Theoretical Physics, University of Cologne, D-50937 Cologne, Germany*

(Dated: November 8, 2018)

We report on a metal-insulator transition in the $\text{LaAlO}_3\text{-SrTiO}_3$ interface electron system, of which the carrier density is tuned by an electric gate field. Below a critical carrier density n_c ranging from $0.5 - 1.5 \times 10^{13}/\text{cm}^2$, $\text{LaAlO}_3\text{-SrTiO}_3$ interfaces, forming drain-source channels in field-effect devices are non-ohmic. The differential resistance at zero channel bias diverges within a 2% variation of the carrier density. Above n_c , the conductivity of the ohmic channels has a metal-like temperature dependence, while below n_c conductivity sets in only above a threshold electric field. For a given thickness of the LaAlO_3 layer, the conductivity follows a $\sigma_0 \propto (n - n_c)/n_c$ characteristic. The metal-insulator transition is found to be distinct from that of the semiconductor 2D systems.

Conducting electron systems with unique properties can be generated at interfaces between highly insulating oxides, the most widely studied case being the interface between the TiO_2 -terminated (001) surface of SrTiO_3 and LaAlO_3 [1]. This electron system behaves as a two-dimensional (2D) electron liquid [2] for which superconducting [3] and magnetic ground states [4] have been reported. At low temperatures, the interface can be tuned from a superconducting to a resistive state by applying transverse electric fields [5]. At higher temperatures, large electric gate fields drive the system through a metal-insulator transition (MIT) [6, 7].

The $\text{LaAlO}_3\text{-SrTiO}_3$ 2D system is disordered [8]; the disorder arising, for example, from dislocations crossing the interface, or from point defects. Consequently, as a 2D electron system (2DES), the interface is expected to be an insulator for $T = 0$, at least for negligible interaction strength among the electrons [9]. The observed metallic behavior may be interaction-driven or a crossover effect; sizable interactions have indeed to be anticipated due to the large interaction energy at small carrier densities [10, 11]. Indeed, for the 2DES of semiconductor interfaces [12, 13] it has been argued [14] that the metallic phase is not a Fermi liquid because a fictitious electron system with suppressed electronic correlations would form a localized phase [9] rather than a 2D Fermi gas. The polar nature of the $\text{LaAlO}_3\text{-SrTiO}_3$ interface possibly results in additional defects and excitations. Excitations of localized electrons and charged defects, for example, can enhance dephasing and thereby reduce weak localization.

The MIT at semiconductor interfaces is still being debated intensely [15–20]. The discovery of a MIT at the interface of perovskite oxides, an entirely different host structure for a 2DES, may shed light on the nature of the MIT in two dimensions. In previous experiments [6, 7] the MIT was deduced from the suppression of the conductance, but has not been investigated further.

In field-effect studies of the perovskite interfaces, the gate fields were considered to change the properties of the

electron system primarily by altering the carrier density n . It has recently been revealed, that by compressing the electron wave function toward the interface, the field also changes the effective disorder of the system and therefore its electronic mobility μ [21].

To advance these issues further, we have measured the current-density vs. electric-field characteristics ($J(E)$) of the interface electron system as a function of applied gate fields. These studies show that in the samples investigated the effects of the gate fields have a strong component that arises from a change of n . The data furthermore reveal a power-law behavior of the conductivity σ of the 2D electron liquid as function of n .

For the measurements we have fabricated seven samples with thicknesses of the LaAlO_3 layers of 4 and 8 unit cells (uc) to investigate a possible dependence of the field effects on the LaAlO_3 thickness. The thickness of 4 uc was chosen to yield the critical thickness required for interface conduction [6]. The samples were fabricated by epitaxially growing LaAlO_3 layers on the (001) surfaces of TiO_2 -terminated [22, 23], 1 mm thick SrTiO_3 single crystals. Scanning force microscopy was used to verify that the substrate surfaces were atomically flat. The films with a nominal composition of LaAlO_3 were grown by pulsed laser deposition from a single crys-

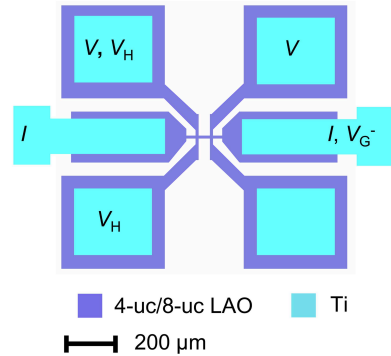


FIG. 1: Sketch of the sample structure (top view).

talline LaAlO₃ target using standard deposition conditions (780 °C, 7×10^{-5} mbar O₂). By reflective high energy electron diffraction the thickness of the LaAlO₃ layers was controlled with a precision of $\sim 0.1 - 0.2$ uc. After growth, the films were annealed for an hour in 400 mbar O₂ to minimize oxygen vacancies. The devices were photolithographically patterned [24] into the structure shown in Fig. 1. This structure was optimized for Hall measurements and for four-point measurements of the $J(E)$ -characteristics, using a small distance between the voltage contacts to minimize the inhomogeneity of the gate fields. Contact pads for the voltage and current leads were prepared by sputtering Ti into holes Ar-ion etched through the LaAlO₃. The back gate was provided by silver diffused into the SrTiO₃.

For each gate voltage (V_G) the $J(E)$ -characteristic in zero magnetic field, Hall voltages and the magnetoconductances at several gate voltages were measured. Gate leakage was always below 1 nA. Only negative gate voltages were applied, for these characteristics were found to be reversible with n .

The $J(E)$ -characteristics are shown in Fig. 2(a). At small J and small $|V_G|$ ($V_G \geq -61.2$ V, 4 K) the characteristics are linear for the whole range of J and for $T < 50$ K. At larger $|V_G|$ ($V_G < -61.2$ V, 4 K), however, the $J(E)$ -characteristics are nonlinear, showing an enhanced differential resistance for small currents. For $V_G < -62.1$ V (inset of Fig. 2(a)), the curves show a clear threshold behavior: below a characteristic threshold field E_{th} , the current density is extremely small ($< 2 \mu\text{A}/\text{cm}$) and shows a weak hysteretic behavior, which is caused by the RC -time constant of the measurement. Because these current densities are minute, we cannot rule out that they are affected by finite gate currents. Above E_{th} the current grows nonlinearly. The width E_{th} diminishes with increasing n to approach zero at a critical density $\sim n_c$ (Fig. 2(b)) defined below.

The conductivity curves bear the characteristic shape shown in Fig. 3(a) for the 4 uc thick samples in zero magnetic field. The 8 uc thick samples display a similar, but noisier behavior (shown in supplement). For $n \geq 2 \times 10^{13}/\text{cm}^2$ the conductivity at zero bias σ_0 decreases approximately linearly with n . As long as the samples show linear [25] $J(E)$ -characteristics, e.g. at $V_G > -61.2$ V (Fig. 2(a)), their conductivities are at least of order e^2/h . Conductivity values with $\sigma_0 \lesssim e^2/h$ that are plotted in Fig. 3(a) were obtained from non-linear characteristics and present the differential conductivity at zero bias (σ_0). For $n < n_c \sim 0.5 - 1.5 \times 10^{13}/\text{cm}^2$ (depending on sample and temperature), however, σ_0 collapses and the samples are effectively insulating (Fig. 2), unless an in-plane electric field $E > E_{th}$ is applied. The transition from the insulating to the linear regime occurs within $\sim 0.02 n_c$ and is reversible with n . The Hall mobility $\mu \equiv \sigma/ne$ is small near the transition, equalling $\sim 30 \text{ cm}^2/\text{Vs}$ and $\sim 5 \text{ cm}^2/\text{Vs}$ as calculated in the linear

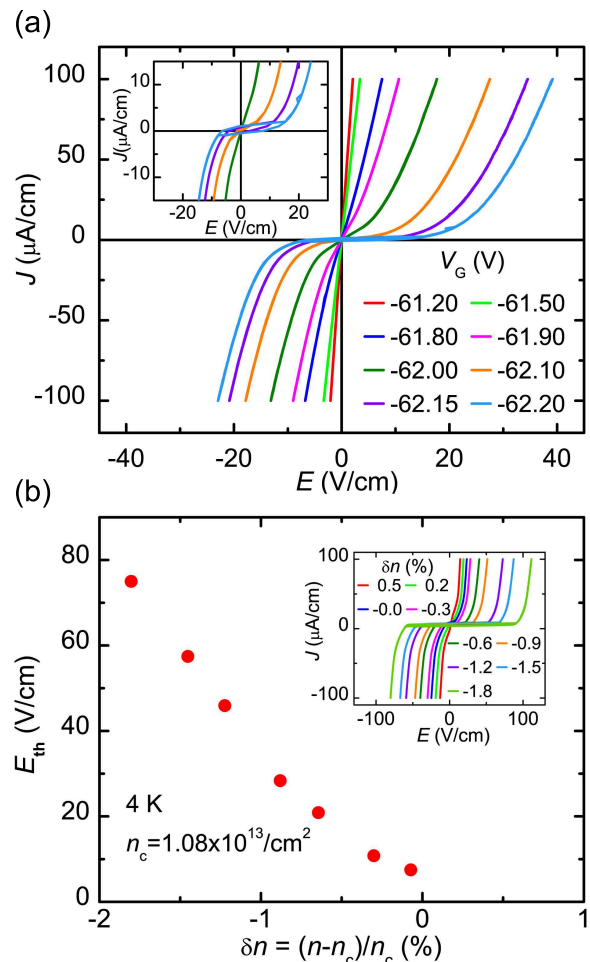


FIG. 2: (a) $J(E)$ -characteristics of a measurement bridge in a LaAlO₃-SrTiO₃ interface with a 4 uc thick LaAlO₃ layer (4 K, no applied magnetic field). The bridge was 60 μm long and 10 μm wide. At $V_G = -61.2$ V, the $J(E)$ -characteristic changes from linear to non-linear behavior with a much smaller conductivity. At $V_G = -62.1$ V, the differential conductivity at $J \sim 0$ equals $\sim 10^{-7}$ S. Below $V_G = -62.1$ V a hysteresis emerges near zero bias (inset) and conductivity sets in only above a threshold field E_{th} . Because in the insulating regime the voltage V along the bridge is no longer small compared to V_G , the respective $J(E)$ -characteristics are asymmetric. (b) Threshold electric field E_{th} plotted as function of the reduced carrier density $\delta n = (n - n_c)/n_c$. The inset shows the respective $J(E)$ curves.

regime for the 4 and 8 uc thick samples, while outside the transition μ reaches $1000 \text{ cm}^2/\text{Vs}$.

Overall, the temperature dependence of the conductivity is surprisingly weak and can, to a large extent, be absorbed into a simple shift of the curves along the n -axis. For all samples of a given thickness we therefore find that the $\sigma(n)$ -characteristics in the ohmic regime can be scaled onto a master curve (Fig. 3(b)). In this figure the conductivity σ_0 is plotted as a function of the reduced carrier density $\delta n = (n - n_c)/n_c$. The values of

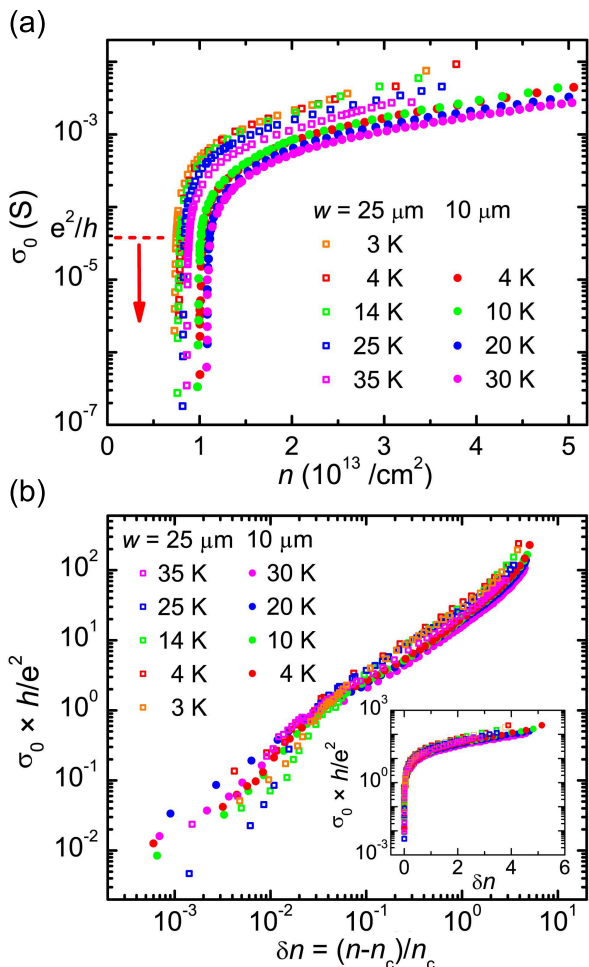


FIG. 3: (a) Conductivities of 10 μm and 25 μm wide channels in 4 uc $\text{LaAlO}_3\text{-SrTiO}_3$ interfaces measured as function of the carrier density varied by V_G (in zero magnetic field). For $\sigma_0 \lesssim e^2/h$, the current-voltage characteristics are non-linear. Only data points derived from $J(E)$ curves that are reversible for the whole bias range are plotted. (b) Conductivities of $\text{LaAlO}_3\text{-SrTiO}_3$ interfaces plotted as function of the reduced carrier density. The scaling curve only includes data points in the ohmic regime. For $\delta n = 0$, σ_0 becomes minute (inset).

n_c depend on temperature and are given in the supplementary materials section. For $0.05 < \delta n < 1$, in this range $\sigma_0 > e^2/h$, the master curve is characterized by a power-law behavior $\sigma_0 \propto \delta n^q$, with $q \sim 1$. Interestingly, the interfaces follow this characteristic curve for the whole temperature range for which the experiments could be performed ($4.2 \text{ K} < T < 50 \text{ K}$), although the dielectric constant of SrTiO_3 is temperature dependent. While the data of the 8 uc samples are characterized by considerably larger scatter, for $0.05 < \delta n < 1$ they approach the curve of the 4 uc thick samples (shown in the supplement).

In the vicinity of the MIT, within a 2% variation of the carrier density, the data scatter more and the zero-bias differential conductivity deviates from a power-law de-

pendence, when $\sigma_0 < e^2/h$. Similarly, on the insulating side a decrease of n by just 1 or 2% causes substantial threshold fields (Fig. 2b).

For an analysis of the behavior close to the MIT, it is suggestive to compare the 2DES of $\text{LaAlO}_3\text{-SrTiO}_3$ interfaces to the 2DES of semiconductor interfaces [12, 13, 15, 19], for which many different scenarios have been discussed, see, e.g., [14–19]. In these semiconductor systems, the transition is controlled by *two* parameters, temperature and density, whose interplay can be described by a single-parameter scaling function, $\sigma(\delta n, T) = f(\delta n/T^{1/\nu z})$, where ν is the correlation length exponent, and z the dynamical critical exponent. These exponents are usually of the order of one. In contrast, the conductivity of the $\text{LaAlO}_3\text{-SrTiO}_3$ interfaces is primarily controlled by δn ; the temperature has very little influence and accordingly such a scaling relation is not found. In this respect, the MIT is not comparable to that of the semiconductor interfaces. Moreover, the $J(E)$ -characteristics for $n < n_c$ display a threshold behavior with a subsequent $J(E) \propto (E - E_{\text{th}})^2$ dependence which has not been observed for the semiconductor interfaces.

Several candidates of possible insulating states exist. The first candidate is an Anderson insulator, in which single electrons are localized by disorder. The second candidate arises, if Coulomb interactions are strong; the electrons then form a Wigner crystal which is pinned by disorder. The third candidate is a polaronic insulator; strong electron-phonon interaction can lead to a self-trapping and localization. One of our surprising results is the absence of significant temperature dependencies of the $J(E)$ -characteristics in combination with strong non-linear effects from moderate electric fields. In a typical electric field of 10 V/cm, an electron has, for example, to travel about 1 μm , more than 100 times the typical distance of electrons at n_c , to gain an energy of $k_B T$ (for $T = 10 \text{ K}$). The effective absence of thermal effects therefore implies that either barriers prohibiting transport are macroscopic in size or that the motion of electrons is controlled by a collective effect in which many electrons participate as is, e.g., the case in a Wigner crystal. Indeed, the characteristic dependence of the conductivity on the electric field is known from the depinning of two-dimensional vortex lattices in superconducting films [26]. Also simple estimates [11] suggest that Coulomb interactions can be sufficiently strong to induce Wigner crystallization, especially if one takes into account that polaronic effects may enhance the tendency to crystallization.

A possible scenario is therefore that at the MIT an insulating phase, such as a pinned Wigner crystal, percolates through the system. Remarkably, the MIT has been related to a percolation transition also in semiconductor systems [16, 20]. The critical conductance exponent of a percolation transition in 2D is 1.3, in conformity with our findings. For the low electronic densities in

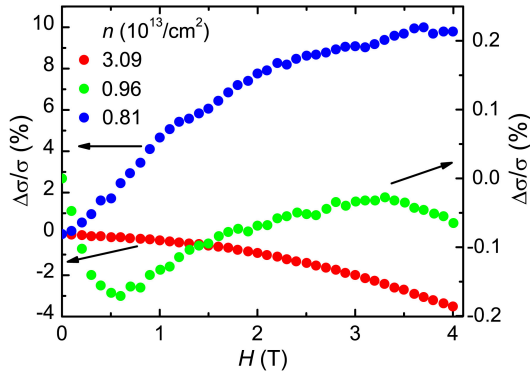


FIG. 4: Magnetoconductance of the 25 μm sample shown in Fig. 3(a) measured at 4.2 K. Due to the large Hall voltage in the depleted state, the conductance is symmetrized using $(\sigma(H) + \sigma(-H))/2$. From high to low carrier density, the corresponding reduced carrier densities, δn , are 2.96, 0.23, and 0.03, respectively.

the semiconductor systems, the transition is possibly induced through scattering by unscreened impurity charges [20]. For the $\text{LaAlO}_3\text{-SrTiO}_3$ 2D system the charge density of order $10^{13}/\text{cm}^2$ is so high that it may preclude the observation of a percolation transition driven by unscreened impurity charges. An alternative possibility is a transition where a Wigner crystal or another phase, e.g., a glassy state induced by strong Coulomb interactions [17], melts. It is also noted that for oxide materials n_c is a small carrier density. The carrier injection induced by a electric field $E > E_{\text{th}}$ causes a non-equilibrium state with a carrier density that is locally enhanced. We therefore regard it as a possibility that the MIT is influenced or even triggered by macroscopic inhomogeneities in the sample and the enhanced carrier density at the contacts. This could also affects the $J(E)$ -dependencies, causing non-linearities.

To illustrate the characteristics of the $\text{LaAlO}_3\text{-SrTiO}_3$ interface above the MIT, typical magnetoconductance curves are shown in Fig. 4. At high carrier density, the $\Delta\sigma/\sigma$ -characteristics exhibit a $-H^2$ dependence (red curve), resembling the typical behavior of metals in small magnetic fields. As revealed in previous studies [5, 27–29], the magnetoconductance of the depleted $\text{LaAlO}_3\text{-SrTiO}_3$ interface shows a negative derivative in low fields and a positive in high fields (green curve). This behavior has been interpreted as the result of spin-orbit interaction and weak localization [29]. Near the MIT, in contrast, the magnetoconductance is always positive and has a negative second derivative in high fields (blue curve).

In summary, the transport properties of $\text{LaAlO}_3\text{-SrTiO}_3$ interfaces were measured as a function of the mobile carrier density altered by gate fields. It is found that below a critical carrier density $n_c \sim 1 \times 10^{13}/\text{cm}^2$

the interfaces become insulating for small in-plane electric field. For samples with 4 uc thick LaAlO_3 layers, this transition occurs at a conductivity of order e^2/h . For a wide range of temperatures, the dependencies of the conductivity on the reduced carrier density follow a $\sigma_0 \propto (n - n_c)/n_c$ characteristic.

While it remains to be explored, which of the proposed microscopic mechanisms, such as disorder potentials or polaronic enhancement of Wigner localization, determine the nature of the MIT, it is evident that the MIT in $\text{LaAlO}_3\text{-SrTiO}_3$ interfaces differs qualitatively from the one in two-dimensional semiconductor systems.

The authors gratefully acknowledge fruitful discussions with T. Nattermann and financial support by the DFG (TRR 80, SFB 608) and the EU (oxIDES).

-
- [1] A. Ohtomo and H. Hwang, *Nature* **427**, 423 (2004).
 - [2] M. Breitschaft *et al.*, *Phys. Rev. B* **81**, 153414 (2010).
 - [3] N. Reyren *et al.*, *Science* **317**, 1196 (2007).
 - [4] A. Brinkmann *et al.*, *Nat. Mat.* **6**, 493 (2007).
 - [5] A. D. Caviglia *et al.*, *Nature* **456**, 624 (2008).
 - [6] S. Thiel *et al.*, *Science* **313**, 1942 (2006).
 - [7] C. Cen *et al.*, *Nature Materials* **7**, 298 (2008).
 - [8] S. Thiel *et al.*, *Phys. Rev. Lett.* **102**, 046809 (2009).
 - [9] E. Abrahams *et al.*, *Phys. Rev. Lett.* **42**, 673 (1979).
 - [10] L. Li *et al.*, arXiv:1006.2847 (2010).
 - [11] At the $\text{LaAlO}_3\text{-SrTiO}_3$ interface, the Fermi energy equals approximately 10 meV [30]. Below 50 K, the oxide interfaces therefore do not reach the Fermi temperature. The kinetic energy per particle is $E_{\text{kin}} \propto n$ and the Coulomb interaction $V \propto n^{1/2}$, so that $V/E_{\text{kin}} \sim 100/\epsilon$. With a dielectric constant $\epsilon \sim 5 - 10$ we conclude that the Coulomb energy exceeds the kinetic energy by an order of magnitude, similar to the semiconductor systems.
 - [12] S. V. Kravchenko *et al.*, *Phys. Rev. B* **51**, 7038 (1995).
 - [13] S. V. Kravchenko and M. P. Sarachik, *Rep. Prog. Phys.* **67**, 1 (2004).
 - [14] V. Dobrosavljević *et al.*, *Phys. Rev. Lett.* **79**, 455 (1997).
 - [15] D. Popović, A. B. Fowler, and S. Washburn, *Phys. Rev. Lett.* **79**, 1543 (1997).
 - [16] Y. Meir, *Phys. Rev. Lett.* **83**, 3506 (1999).
 - [17] A. A. Pastor and V. Dobrosavljević, *Phys. Rev. Lett.* **83**, 4642 (1999).
 - [18] B. L. Altshuler and D. L. Maslov, *Phys. Rev. Lett.* **82**, 145 (1999).
 - [19] S. Washburn *et al.*, *Ann. Phys.* **8**, 569 (1999).
 - [20] L. A. Tracy *et al.*, *Phys. Rev. B* **79**, 235307 (2009).
 - [21] C. Bell *et al.*, *Phys. Rev. Lett.* **103**, 226802 (2009).
 - [22] M. Kawasaki *et al.*, *Science* **266**, 1540 (1994).
 - [23] G. Koster *et al.*, *Appl. Phys. Lett.* **73**, 2920 (1998).
 - [24] C. W. Schneider *et al.*, *Appl. Phys. Lett.* **89**, 122101 (2006).
 - [25] We use the word “ohmic” following the usage to describe $J(E)$ characteristics with a finite conductance at $E = 0$. $J(E)$ characteristics in which $J \propto E$ are called “linear”.
 - [26] P. H. Kes and C. C. Tsuei, *Phys. Rev. B* **28**, 5126 (1983).
 - [27] C. Bell *et al.*, *Appl. Phys. Lett.* **94**, 222111 (2009).
 - [28] M. Ben Shalom *et al.*, *Phys. Rev. Lett.* **104**, 126802

(2010).
[29] A. D. Caviglia *et al.*, Phys. Rev. Lett. **104**, 126803
(2010).

[30] This applies for $n \sim 10^{13}/\text{cm}^2$ and $m^*/m_e \sim 3$.